Ab Initio/Density Functional Theory and Multichannel RRKM Study for the ClO + CH_2O Reaction

Yan Tian, Wen-Mei Wei, Zhi-Mei Tian, Hong-Yi Yang, Tian-Jing He,* Fan-Chen Liu, and Dong-Ming Chen

Department of Chemical Physics, University of Science and Technology of China, Hefei, Anhui 230026 P.R. China

Received: March 2, 2006; In Final Form: July 10, 2006

The potential energy surface for the CH_2O + ClO reaction was calculated at the QCISD(T)/6-311G(2d,2p)//B3LYP/6-311G(d,p) level of theory. The rate constants for the lower barrier reaction channels producing HOCl + HCO, H atom, OCH_2OCl, *cis*-HC(O)OCl and *trans*-HC(O)OCl have been calculated by TST and multichannel RRKM theory. Over the temperature range of 200−2000 K, the overall rate constants were $k(200-2000K) = 1.19 \times 10^{-13}T^{0.79} \exp(-3000.00/T)$. At 250 K, the calculated overall rate constant was 5.80×10^{-17} cm^3 molecule^{-1} s^{-1}, which was in good agreement with the experimental upper limit data. The calculated results demonstrated that the formation of HOCl + HCO was the dominant reaction channel and was exothermic by 9.7 kcal/mol with a barrier of 5.0 kcal/mol. When it retrograded to the reactants CH_2O + ClO, an energy barrier of 14.7 kcal/mol is required. Furthermore, when HOCl decomposed into H + ClO, the energy required was 93.3 kcal/mol. These results suggest that the decomposition in both the forward and backward directions for HOCl would be difficult in the ground electronic state.

1. Introduction

Formaldehyde (CH_2O) is an important intermediate in the oxidation of alcohols, ethers, and hydrocarbons in general,[1,2] and it is, in particular, a significant pro-knock additive of the methane-base fuel.[3,4] Moreover, the thermodynamic stability of formaldehyde leads to large accumulation in air and final pollution, and it causes a concern environmentally.[5] One important question is whether it can react with some radicals such as ClO_x radical to form stable products. There have been extensive experimental studies on the kinetics of reactions for ClO_x and atmospheric species in conjunction with the computer simulation of ozone depletion by freons.[6−9] As we all know that ClO is one of the main products of CFCs photolysis in atmosphere. A recent study of the ignition and combustion for ammonium per chlorate in atmosphere showed that ClO radicals were generated at 1400 K near the burner surface at the same level of concentration as the OH radicals.[10] ClO is known to play an important role in the ozone depletion cycle in atmosphere.[11] Recent studies in the Arctic have shown a correlation between the concentration of formaldehyde (CH_2O) and that of ozone.[12]

It is well-known that hypochlorous acid (HOCl) has been recognized as a temporary reservoir for ClO_x species in stratosphere.[13−16] To evaluate whether HOCl and HCO are the main products in the reaction of ClO + CH_2O, it is important to understand the mechanisms and kinetics of this reaction in atmosphere.

To our knowledge, a few determinations of the rate constant for the reaction CH_2O + ClO → products have been published in the literature. In 1980, Poulet et al.[17] studied the kinetics of this reaction using the discharge flow-EPR technique and reported an upper limit of the rate constant at 298 K ($k < 1.0 \times 10^{-15}$ cm^3 molecule^{-1} s^{-1}). They suggested the possible reaction be CH_2O + ClO → HOCl + HCO. On the basis of these data, DeMore et al.[18] have estimated the rate expression over the temperature range 200−300 K. $k = 1.0 \times 10^{-12}$ (cm^3 molecule^{-1} s^{-1}) × exp (−4.17 (kcal mol^{-1})/*RT*), where the activation energy is assumed to be a lower limit.

In this work, we used high-level ab initio molecular orbital methods to investigate the reaction between CH_2O and ClO and attempted to map out the complete potential energy surface (PES) for this system. On the basis of the computed PES, we carried out the total rate constant and branching ratio calculations of this reaction using the multichannel RRKM and variational transition state methods.

2. Computational Methods

The geometry of the reactants, products, intermediates, and transition states of the reaction CH_2O + ClO have been fully optimized by using the hybrid density functional B3LYP method (Becke's three-parameter exchange functional with the correlation functional of Lee, Yang, and Parr[19−22]) with the standard 6-311G(d,p) basis set. Vibrational frequencies have been calculated at the same level to determine the nature and zero-point energy (ZPE) corrections of the stationary points, and have been used for the rate constant calculations. Each saddle point was verified to connect the proper reactants and products by performing an intrinsic reaction coordinate (IRC[23]) calculation. The geometries optimized at the B3LYP/6-311G(d,p) level were used to perform single point energy calculations for all species at the quadratic configuration interaction level of theory using single, double, and triple excitations (QCISD(T)),[24] with the basis set of 6-311G(2d,2p). In this work, we have also carried out additional calculations in some cases using CCSD(T)/6-311G(2d,2p) and G2MP2/B3LYP methods to confirm the energies obtained by the QCISD(T)/6-311G(2d,2p) method. Our

* Corresponding author. Fax: +86−551−3603388. E-mail: tj16@ustc.edu.cn.

10.1021/jp061314x CCC: $33.50
Published on Web 09/06/2006

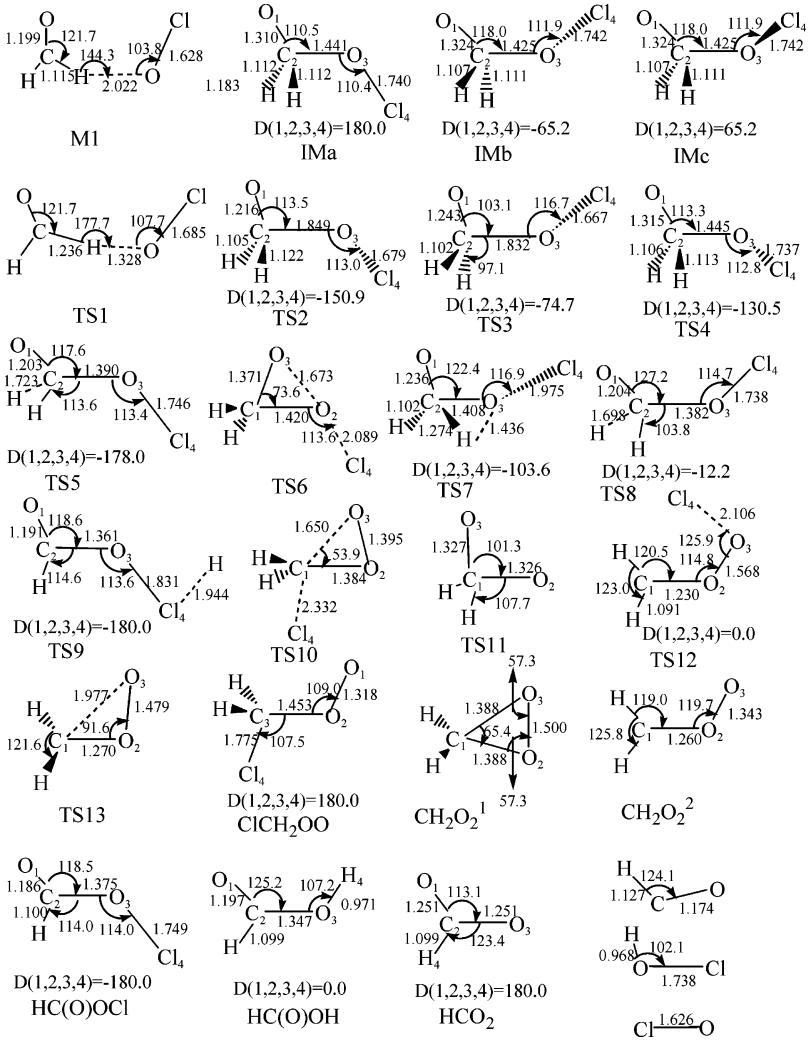

Figure 1. Optimized structures of various species involved in the reaction of CH_2O with ClO. Bond distances are in angstroms and angles are in degree.

calculations indicate that the barriers calculated using these three methods for the main reaction channels are in good agreement with each other. All calculations were performed with the GAUSSIAN 98 package.[25]

3. Results and Discussion

The optimized geometries of the intermediates and transition states are shown in Figure 1. The overall energy profile based on the QCISD(T)/6-311G(2d,2p)//B3LYP/6-311G(d,p) method is depicted in Figure 2. Table 1 summarizes the electronic energies calculated by three different methods. The vibrational frequencies and moments of inertia for the species used in the rate-constants calculations are summarized in Table 2.

3.1. Potential Energy Surface and Reaction Mechanisms. *(a) HOCl + HCO Formation.* The calculated results showed this reaction is a hydrogen abstraction process. The first step of the ClO radical approaching the hydrogen atom of CH_2O involves the formation of a molecular complex (M1, in Figure 1). All the vibrational frequencies of M1 are positive, which indicates the molecular complex M1 is a stable structure. The molecular complex M1 lies approximately 1.4 kcal/mol below the reactants at the QCISD(T)/6-311G(2d,2p) level of theory. The energies of the complex at different levels of theory are shown in Table 1. This complex is characterized by an intermoiety distance of 2.022 Å, owing to the long-range interactions between the CH_2O molecule and the ClO radical. This is very similar to the reaction of BrO radical with CH_2O molecule,[12] where the formed CH_2O-BrO complex possessed an OH distance of 2.571 Å. When the ClO radical is getting closer to the hydrogen atom of the CH_2O molecule, the transition state TS1 is located, which connects the complex M1with the products HOCl + HCO (P1). In TS1, the breaking C−H bond is elongated to 1.236 Å, which is only 11% longer than the C−H bond in CH_2O. On the contrary, the distance between the O atom of the ClO radical and the H atom of the CH_2O molecule is shortened to 1.328 Å, and it is 0.36 Å longer than the O−H bond in the HOCl molecule. The relative energy calculated at QCISD(T) level of theory for TS1 is 5.0 kcal/mol higher than that of the reactants CH_2O + ClO, while the relative energies calculated at the CCSD(T) and G2MP2/B3LYP levels of theory for TS1 are 5.9, 6.2 kcal/mol, respectively. Our calculation is consistent with the result of Poulet et al.[17] They reported that the barrier should be higher than 4.2 kcal/mol for the formation of HOCl + HCO process. The energy of the products P1(HOCl + HCO) is 9.7 kcal/mol lower than that of the reactants.

(b) OCH_2OCl Intermediate and the Related Isomerization and Decomposition. The O atom of the OCl radical attacks the C atom of the CH_2O molecule in the vertical direction of the CH_2O molecule plane to form intermediate IMa (OCH_2OCl) via a transition state TS2. In TS2, the forming C−O bond is 1.849 Å and the C−O bond of CH_2O is slightly stretched by 0.016 Å. The energy of TS2 is 18.3 kcal/mol higher than that of the

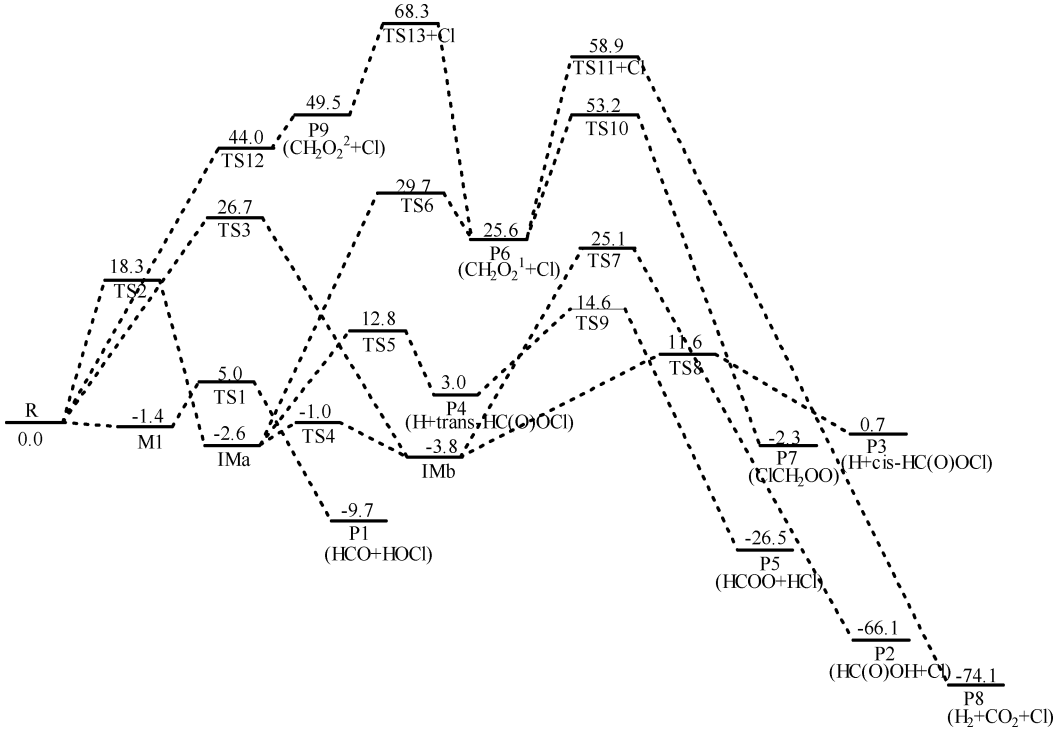

Figure 2. Profile of potential energy surface for the CH_2O + ClO reaction. Relative energies are calculated at the QCISD(T)/6-311G(2d,2p)// B3LYP/6-311G(d,p) level.

TABLE 1: Relative Energies (RE, kcal mol^{-1}) at the Different Levels of Theory and ZPE Corrections (kcal mol^{-1}) at the B3LYP/6-311G(d,p) Level of Theory for Species Involved in the Reaction of CH_2O + ClO

species	ZPE[a]	RE1	RE2	RE3
CH_2O + CLO[b]	17.1	0.0	0.0	0.0
M1	17.8	−1.4	−0.5	−0.9
IM1a	19.1	−2.6	−2.7	−3.3
IM1b	19.4	−3.8	−3.8	−4.0
IM1c	19.4	−3.8		
TS1	14.9	5.0	5.9	6.2
TS2	17.7	18.3	18.4	17.9
TS3	18.2	26.7	22.8	23.2
TS4	19.0	−1.0	−1.2	−1.7
TS5	14.9	12.8	13.5	10.4
TS6	19.5	29.7		
TS7	15.9	25.1	27.2	27.3
TS8	15.0	11.6	12.0	9.53
TS9	14.5	14.6		
TS10	19.2	53.2		
TS11 + Cl	16.1	58.9	58.9	62.3
TS12	18.2	44.0	49.8	49.7
TS13 + Cl	17.8	68.3	72.4	62.3
HCO + HOCl	15.6	−9.7	−8.2	−8.9
HCOOH + Cl	20.4	−66.1	−63.2	−68.6
H + *cis*-HC(O)OCl	14.0	0.7	1.4	1.3
H + *trans*-HC(O)OCl	13.8	3.0		
HCO_2 + HCl	15.8	−26.5	−22.7	−24.3
$CH_2O_2{}^1$+Cl	19.5	25.6	26.6	28.5
$ClCH_2OO$	20.5	−2.3		
H_2 + CO_2 + Cl	13.1	−74.1	−69.0	−69.0
$CH_2O_2{}^2$+Cl	18.7	49.5		

[a] Scaled by a factor of 0.96. [b] The energy is −648.93977 hartree at QCISD(T) level. RE1, at QCISD(T) level. RE2, at CCSD(T) level. RE3, at G2MP2/B3LYP level.

reactants CH_2O + ClO at the QCISD(T) level. This reaction is exothermic by 2.6 kcal/mol.

Besides the IMa structure, there are two other isomers, IMb and IMc, and they are the rotational isomers of IMa, which are produced by a rotation around the ClO−OC bond. The energies of IMa, IMb and IMc are −2.6, −3.8 and −3.8 kcal/mol, respectively. In Figure 1, it is very clear that IMb and IMc are the enantiomers about the $O_1-C_2-O_3$ plane and they have the same electronic structures and energies. Thus, in the following discussions we mainly study pathways via isomers IMa and IMb, respectively. Isomer IMa can isomerize to isomer IMb via a transition state TS4 with a barrier of 1.6 kcal/mol. Isomer IMb can also be achieved from the reactants via a transition state TS3 with a barrier height of 26.7 kcal/mol, which suggests that it is not easy for this process to take place at room temperature.

Isomer IMa has two unimolecular decomposition pathways. One is the formation channel of H + *trans*-HC(O)OCl (P4) via a transition state TS5. The breaking C−H bond in TS5 is elongated by 0.611 Å, while the $C-O_1$ and $C-O_3$ bonds are shortened to 1.203 and 1.390 Å, respectively. The product P4 can further transform to more stable products HCO_2 + HCl (P5) via the transition state TS9. The relative energies of TS5, P4, TS9, and P5 are 12.8, 3.0, 14.6, and −26.5 kcal/mol, respectively. The other pathway is the formation of the product P6 (Cl atom and a ring-structure molecule $CH_2O_2{}^1$) via a three-member-ring transition state TS6 with a barrier of 32.3 kcal/mol. In TS6, the forming O_2-O_3 bond is shortened to 1.673 Å, while the breaking O_2-Cl bond is elongated from 1.740 to 2.089 Å. Owing to the higher barrier height for this process, this channel does not play an important role in the overall reaction.

IMb also has two decomposition pathways. As shown in Figure 2, the first decomposition channel is the formation of Cl + HC(O)OH (P2) via a transition state TS7 with a barrier of 28.9 kcal/mol. In this process, with the stretching of the O_3-Cl bond one of the H atom shifts form C atom to O_3 atom and forms a new O−H bond.

The second dissociation channel of IMb is that leading to the production of H + *cis*-HC(O)OCl (P3) via a transition state TS8 with a barrier of 15.4 kcal/mol. The relative energy of TS8 is 11.6, 12.0, and 9.53 kcal/mol by using QCISD(T), CCSD-(T), and G2MP2/B3LYP methods, respectively.

(c) Direct Oxygen Abstraction Channel. The calculation result indicates that there is a direct oxygen abstraction channel. The

TABLE 2: Vibrational Frequencies (cm^{-1}) and Moments of Inertia (amu) for Various species for the $CH_2O + ClO$ Reaction at the B3LYP/6-311G(d,p) Level of Theory

species	frequencies	I_A, I_B, I_C
CH_2O	1201, 1270, 1539, 1826, 2874, 2923	1.8, 13.0, 14.7
ClO	793	29.1
M1	69, 71, 131, 174, 194, 783, 1197, 1256, 1516, 1823, 2808, 2915	40.8, 191.3, 232.1
IMa	106, 270, 434, 720, 731, 973, 1137, 1164, 1306, 1357, 2840, 2850	12.5, 181.2, 190.5
IMb	126, 290, 586, 634, 809, 938, 1117, 1180, 1312, 1344, 2864, 2930	30.5, 137.1, 158.1
IMc	126, 290, 586,633, 809, 939, 1116, 1181, 1312, 1344, 2864, 2930	
TS1	850*i*, 57, 72, 331, 337, 607, 887, 1134, 1202, 1506, 1885, 2844	35.7, 209.4, 245.1
TS2	552*i*, 104, 191, 389, 692, 713, 1036, 1120, 1372, 1594, 2722, 2930	15.8, 203.5, 212.7
TS3	728*i*, 90, 197, 303, 671, 815, 1111, 1192, 1419, 1528, 2925, 2991	
TS4	114*i*, 316, 452, 674, 783, 932, 1113, 1165, 1308, 1333, 2845, 2920	17.0, 177.8, 181.3
TS5	958*i*, 144, 289, 473, 497, 546, 745, 1028, 1069, 1341, 1716, 2984	13.0, 179.3, 187.1
TS6	578*i*, 183, 236, 406, 857, 1061, 1187, 1249, 1299, 1552, 3046, 3135	
TS7	1657*i*, 122, 221, 374, 610, 637, 908, 1060, 1320, 1498, 1864, 2981	
TS8	988*i*, 217, 244, 484, 570, 629, 783, 977, 1056, 1312, 1708, 2974	32.1, 126.3, 152.4
TS9	1237*i*, 35, 169, 260, 456, 575, 703, 1032, 1101, 1384, 1833, 3024	
TS10	1073*i*, 173, 238, 282, 878, 963, 1087, 1164, 1220, 1469, 3159, 3326	
TS11	1327*i*, 818, 835, 1098, 1181, 1208, 1318, 2610, 2657	
TS12	702*i*, 118, 141, 367, 495, 518, 1127, 1228, 1447, 1632, 3040, 3176	
TS13	697*i*, 740, 776, 1014, 1199, 1406, 1556, 3053, 3211	

O atom in ClO radical is abstracted by the oxygen atom in CH_2O, forming a linear-structure molecule $CH_2O_2^2$ and Cl atom (P9), via a transition state TS12, and furthermore, the linear-structure molecule $CH_2O_2^2$ can isomerize to $CH_2O_2^1$ via a transition state TS13. The relative energies of TS12 and TS13 + Cl are 44.0 and 68.3 kcal/mol, respectively. From Figure 2 we can see that, $CH_2O_2^1$ can react with Cl atom to form $ClCH_2$-OO (P7) via a transition state TS10 with a barrier of 27.6 kcal/mol. Besides this, the $CH_2O_2^1$ molecule can also decompose to the final products CO_2 and H_2 via a transition state TS11with a barrier of 33.3 kcal/mol.

3.2. Rate Constant Calculations. In the formation process of HOCl + HCO, the first step is to form the complex M1 with a energy decline of 1.4 kcal/mol, and then, it is followed by an internal rearrangement with a barrier of 6.4 kcal/mol to obtain the products HOCl + HCO. Owing to the larger energy difference between these two reaction steps, the preequilibrium approximation holds good in this case.[26] On the basis of the steady-state analysis, the rate constant for the above reaction was calculated, and a semiclassical one-dimensional multiplicative tunneling correction factor[27] was also used to predict the temperature dependence of the rate constant (k_1).

$$k_{eq} = \frac{Q_{M1}}{Q_{CH_2O}Q_{ClO}}\exp\left(-\frac{E_{M1}-E_R}{RT}\right) \quad (1)$$

$$k_d(T) = \Gamma(T)\frac{k_bT}{h}\frac{Q_{TS}}{Q_{M1}}\exp\left(-\frac{E_{TS}-E_{M1}}{RT}\right) \quad (2)$$

$$k1(T) = k_{eq}k_d(T) = \Gamma(T)\frac{k_bT}{h}\frac{Q_{TS}}{Q_{CH_2O}Q_{ClO}}\exp\left(\frac{E_R-E_{TS}}{RT}\right) \quad (3)$$

$$\Gamma(T) = 1 + \frac{1}{24}\left(\frac{h\upsilon^{\neq}}{k_bT}\right)^2 \quad (4)$$

where $\Gamma(T)$ is the transmission coefficient to correct the tunneling effect at temperature T, and $\upsilon^{\neq}$ is the imaginary frequency at the saddle point. Q_{TS}, Q_{M1}, Q_{CH_2O}, and Q_{ClO} are the total partition functions for the transition state TS1, complex M1, and reactants CH_2O and ClO at temperature T, respectively. E_R, E_{TS} and E_{M1} are the total energies of the reactants, transition state TS1, and complex M1, respectively. k_b is Boltzman's constant, and h is Planck's constant.

The rate constants of the following reaction channels with lower barriers have been calculated using themultichannel RRKM theory.[28]

$$CH_2O + ClO \underset{1}{\overset{a}{\rightleftarrows}} IMa^* \xrightarrow{2} H + \textit{trans}\text{-}HC(O)OCl$$

$$\underset{4}{\overset{3}{\rightleftarrows}} IMb^* \xrightarrow{5} H + \textit{cis}\text{-}HC(O)OCl$$

$$\xrightarrow{\omega 2} IMb$$

$$\xrightarrow{\omega 1} IMa$$

Steady-state assumption for all the excited intermediates leads to the following second-order rate constants of various reaction channels.

$$k2(T) = \frac{\alpha}{h}\frac{Q_{tr}^{\neq}}{Q_{CH_2O}Q_{ClO}}e^{-E^0/(k_bT)} \int_0^{\infty}\frac{k2(E)+k5(E)X2(E)}{Y(E)}W_1(E^{\neq})e^{-E^{\neq}/(k_bT)}\,dE^{\neq} \quad (5)$$

$$k3(T) = \frac{\alpha}{h}\frac{Q_{tr}^{\neq}}{Q_{CH_2O}Q_{ClO}}e^{-E^0/(k_bT)}\int_0^{\infty}\frac{k2(E)}{Y(E)}W_1(E^{\neq})e^{-E^{\neq}/(k_bT)}\,dE^{\neq} \quad (6)$$

$$k4(T) = \frac{\alpha}{h}\frac{Q_{tr}^{\neq}}{Q_{CH_2O}Q_{ClO}}e^{-E^0/(k_bT)}\int_0^{\infty}\frac{k5(E)X2(E)}{Y(E)}W_1(E^{\neq})e^{-E^{\neq}/(k_bT)}dE^{\neq} \quad (7)$$

$$k5(T) = \frac{\alpha}{h}\frac{Q_{tr}^{\neq}}{Q_{CH_2O}Q_{ClO}}e^{-E^0/(k_bT)}\int_0^{\infty}\frac{\omega 1}{Y(E)}W_1(E^{\neq})e^{-E^{\neq}/(k_bT)}\,dE^{\neq} \quad (8)$$

$$k6(T) = \frac{\alpha}{h}\frac{Q_{tr}^{\neq}}{Q_{CH_2O}Q_{ClO}}e^{-E^0/(k_bT)}\int_0^{\infty}\frac{X2(E)\omega 2}{Y(E)}W_1(E^{\neq})e^{-E^{\neq}/(k_bT)}\,dE^{\neq} \quad (9)$$

$$\omega = \beta Z_{LJ}[M] \quad (10)$$

$$X1(E) = k1(E) + k2(E) + k3(E) + \omega 1 \quad (11)$$

$$X2(E) = k3(E)/[k4(E) + k5(E) + \omega 2] \quad (12)$$

$$Y(E) = X1(E) - k4(E)X2(E) \quad (13)$$

$$ki(E) = \alpha i\frac{CiWi(E_i^{\neq})}{h\rho(E)} \quad (14)$$

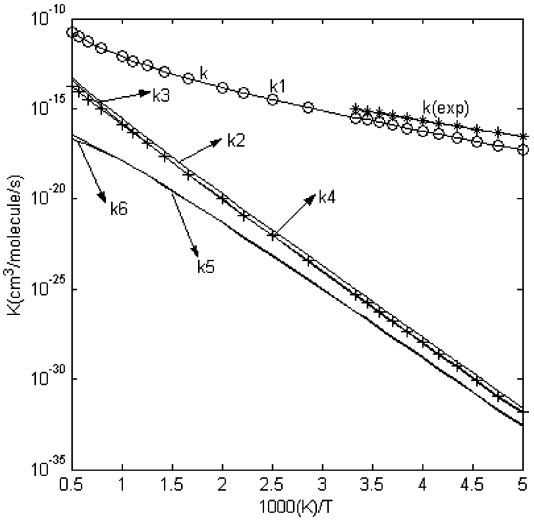

Figure 3. Total and individual rate constants for the CH_2O + ClO reaction. Stars (k_{exp}) correspond to the experimental upper limit data from ref 18.

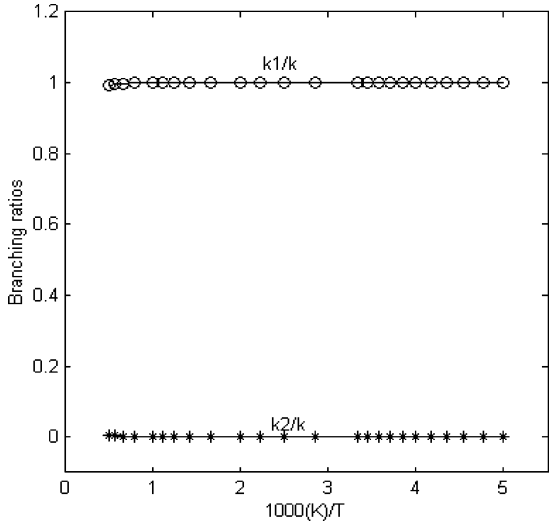

Figure 4. Branching ratios over the temperature range of 200−2000 K for the formation of HOCl + HCO (k1/k) and H atom channels (k2/k).

In the above equations, α (α = 2) is the statistical factor for the reaction path a, and α*i* is the statistical factor for the *i*th (*i* = 1, 2, 3, 4, 5) reaction path,[28] the values of α*i* are 2, 2, 2, 1, and 1, respectively. E° is the energy barrier for the formation of the IMa via the transition state TS2. $Q^{\neq}_{tr}$ is the product of the translational and rotational partition functions of the transition state TS2, and $W_1(E^{\neq})$ is the sum of states the transition state TS2 with excess energy $E^{\neq}$ above the association barrier. k*i*(E) is the energy-specific rate constant for the *i*th channel, and C*i* is the ratio of the overall rotational partition function (symmetry number is not included) of the transition states TS and the reactant in channel *i*, that is, TS2 and IMa, TS5 and IMa, TS4 and IMa, TS4 and IMb, and TS8 and IMb for channel *i* = 1, 2, 3, 4, and 5, respectively, and the values of C*i* are 1.2607, 1.0054, 1.1280, 0.9112 and 0.9667, respectively. The sum of states $Wi(E^{\neq}_i)$ and the density of states ρ(E) were calculated by the Beyer−Swinehart algorithm.[29,30] The rate constant for stabilization of the excited adduct IMa or IMb is given by ω in eq 10 and β is the collision efficiency calculated using Troe's β approximation,[31] in this work β = 0.7. Z_{LJ} is the Lennard-Jones collision frequency,[32] and [M] is the concentration of the bath gas M. k2(T), k3(T), k4(T), k5(T), and k6(T) represent the rate constants of formation of H atom, *trans*-HC(O)OCl, *cis*-HC(O)OCl, IMa, and IMb, respectively.

The total second-order rate constantfor the CH_2O + ClO reaction is given by

$$k(T) = k1(T) + k2(T) + k3(T) + k4(T) + k5(T) + k6(T)$$

The branching ratios are k*i*/k. Figure 3 shows the total and individual rate constants at the temperature range of 200−2000 K and at a pressure of 760 Torr, and the branching ratios for some important channels are depicted in Figure 4.

From Figure 3 we can see that, in the temperature range of 200−300 K, the reaction is dominated by the HOCl + HCO formation channel. At 250 K, the calculated total rate constant is 5.80×10^{-17} cm^3 molecule^{-1} s^{-1}, which is in good agreement with the experimental upper limit value of 2.25×10^{-16} cm^3 molecule^{-1} s^{-1}. [18]

Since the formation of IMa has a higher energy barrier, its multichannel RRKM rate constants are much lower than k1 at the lower temperature region, and the consumption of the reactants is primarily due to the formation of HOCl + HCO. When the temperature is elevated to 2000 K, k1 is still several orders of magnitude higher than k2. As a result, the formation of HOCl + HCO dominates the whole reaction at the temperature range 200−2000 K. Form Figure 3 we can see that the total rate constant is nearly equals to the rate constant k1, and the branching ratios in Figure 4 also indicate that the k1/k is approximately 100%. On the contrary, the branching ratio of k2 is lower than 0.1% between 200 and 2000 K. This is in good agreement with the experimental observation that HOCl + HCO are the major products. It can be noticed from Figure 3 that with the increase of temperature k2, k3 and k4 have a more rapid increase than k1. Then we estimated that, when the temperature is higher than 3000 K, the formation of H atom, *cis*-HC(O)OCl and *trans*-HC(O)OOCl will become competitive with the formation of HOCl + HCO.

The calculated rate constants exhibit a typical non-Arrhenius behavior. This non-Arrhenius behavior has frequently been observed in radical-molecule reactions studied over wide temperature ranges.[33] The calculated rate constants are fitted to a three-parameter formula over the temperature range of 200−2000 K and are given in units of cm^3 molecule^{-1} s^{-1} as follows:

$$k1(200-2000\ \mathrm{K}) = 2.99 \times 10^{-13} T^{0.60} \exp\left(-\frac{3014.99}{T}\right)$$

$$k(200-2000K) = 1.19 \times 10^{-13} T^{0.79} \exp\left(-\frac{3000.00}{T}\right)$$

The calculation results showed that the formation of HOCl and HCO is the major reaction channel in the CH_2O + ClO reaction. When the HCO + HOCl product retrogrades to the reactants CH_2O + ClO, an energy barrier of 14.7 kcal/mol is required. Furthermore, the calculated H−OCl bond dissociation energy is 93.3 kcal/mol at the QCISD(T)/6-311G(2d,2p) level of theory and the enthalpy change of HOCl decomposition to H + ClO at 298 K is 94.3 kcal/mol based on the enthalpy values of JPL 02−25.[34] These results suggest that the decomposition in both the forward and backward directions for HOCl be difficult in the ground electronic state. Thus, HOCl can be considered as a rather good sink for ClO radical, which is in line with the previous studies.[13−16] For that reason, CH_2O can act as an elimination agent for ClO radical by the formation of HOCl molecule.

4. Conclusion

The potential energy surface for the $CH_2O + ClO$ reaction was calculated at the QCISD(T)/6-311G(2d,2p)//B3LYP/6-311G(d,p) level of theory. The rate constants for the lower barriers reaction channels producing HOCl + HCO, H atom, OCH_2OCl, *cis*-HC(O)OCl and *trans*-HC(O)OCl have been calculated by TST and multichannel RRKM theory. Over the temperature range of 200−2000 K, the rate constants for the channel of formation of HOCl + HCO are

$$k1(200-2000\ \mathrm{K}) = 2.99 \times 10^{-13} T^{0.60} \exp\left(-\frac{3014.99}{T}\right)$$

while the overall rate constants are

$$k(200-2000\ \mathrm{K}) = 1.19 \times 10^{-13} T^{0.79} \exp\left(-\frac{3000.00}{T}\right)$$

At 250 K, the calculated overall rate constant is 5.80×10^{-17} cm^3 $molecule^{-1}$ s^{-1}, which is in good agreement with the experimental upper limit value of 2.25×10^{-16} cm^3 $molecule^{-1}$ s^{-1} .[18] Furthermore, over the temperature range 200−300 K the calculated rate constants are also consistent with the experimental upper limit data.

The calculated results demonstrated that the formation of HOCl + HCO is the dominant reaction channel over the temperature range of 200−3000 K; in the same way, the experimental observation indicated that the HOCl + HCO are the main products. The energy of HOCl + HCO is about 9.7 kcal/mol lower than that of reactants, and a barrier of 6.4 kcal/mol is required to produce HOCl + HCO. When the HCO + HOCl product retrogrades to the reactants $CH_2O + ClO$, an energy barrier of 14.7 kcal/mol is required. Furthermore, when HOCl decomposes into H + ClO, the energy required is 93.3 kcal/mol at the QCISD(T)/6-311G(2d,2p) level of theory. These results suggest that the decomposition in both the forward and backward directions for HOCl be difficult in the ground electronic state. Thus, CH_2O can be considered as a sink for ClO radical.

Acknowledgment. This work was supported by the National Natural Science Foundation of China (Grant No. 20473078).

References and Notes

(1) Westbrook, C. K.; Dryer, F. L. *Combust. Sci. Technol.* **1979**, *20*, 125.
(2) Choudhury, K. T.; Lin, M. C. *Combust. Sci. Technol.* **1989**, *64*, 19.
(3) Norton, T. S.; Dryer, F. L. *Combust. Sci. Technol.* **1989**, *63*, 107.
(4) Hunter, T. B.; Wang, H.; Litzinger, T. A.; Frenklach, M. *Combust. Flame* **1994**, *97*, 201.
(5) Zabarnick, S.; Fleming, J. W.; Lin, M. C. *Int. J. Chem. Kinet.* **1988**, *20*, 117.
(6) Rowland, F. S. *Annu. Rev. Phys. Chem.* **1991**, *42*, 731.
(7) Johnston, H. S. *Annu. Rev. Phys. Chem.* **1992**, *43*, 1.
(8) He, T.-J.; Chen, D.-M.; Liu, F.-C.; Sheng, L.-S *Chem. Phys. Lett.* **1999**, *332*, 545.
(9) Wei, W.-M.; Tan, W.; He, T.-J.; Chen, D.-M.; Liu, F.-C *Chin. J. Chem. Phys.* **2004**, *17*, 679.
(10) Yuasa, S.; Yushina, S.; Uchida, T.; Shiraishi, N. *Proc. Combust. Inst.* **2000**, *28*, 863.
(11) Schnell, M.; Muhlhauser, M.; Peyerimhoff, S. D. *J. Phys. Chem. A* **2004**, *108*, 1298.
(12) Hansen, J. C.; Li, Y.-M.; Francisco, J. S. *J. Phys. Chem. A* **1999**, *103*, 8543.
(13) Scientific Assessment of Ozone Depletion, 1994; WMO Global Ozone Research Monitoring Project, Report 37, 1995.
(14) Yung, Y. L.; Pinto, J. P.; Watson, R. T.; Sander, S. P. *J. Atmos. Sci.* **1980**, *37*, 339.
(15) Poulet, G.; Pirre, M.; Maguin, F.; Ramaroson, R.; LeBras, G. *Geophys. Res. Lett.* **1992**, *19*, 2305.
(16) Garcia, R. R.; Solomon, S. J. *Geophys. Res.* **1994**, *99*, 937.
(17) Poulet, G.; Le Bras, G.; Combourieu, J. *Geophy. Res. Lett.* **1980**, *7*, 413.
(18) DeMore, W. B.; Sander, S. P.; Golden, D. M.; Hampson, R. F.; Kurylo, M. J.; Howard, C. J.; Ravishankara, A. R.; Kolb, C. E.; Molina, M. J. *Chemical Kinetics and Photochemical Data for Use in Stratospheric Modeling*; JPL Publication 97−4; NASA: Pasadena, CA, 1997.
(19) Becke, A. D. *J. Chem. Phys.* **1992**, *96*, 2155.
(20) Becke, A. D. *J. Chem. Phys.* **1992**, *97*, 9173.
(21) Becke, A. D.*J. Chem. Phys.* **1993**, *98*, 5648.
(22) Lee, C.; Yang, W.; Parr, R. G. *Phys. Rev. B* **1988**, *37*, 785.
(23) Gonzalez, C.; Schlegel, H. B. *J. Chem. Phys.* **1989**, *90*, 2154.
(24) Pople, J. A.; Head-Gordon, M.; Raghavachari, K. *J. Chem. Phys.* **1987**, *87*, 5968.
(25) Frisch, M. J.; et al. *GAUSSIAN 98*; Gaussian Inc.: Pittsburgh, PA, 1998.
(26) Alvarez-Idaboy, J. R.; Mora-Diez, N.; Boyd, R. J.; Vivier-Bunge, A. *J. Am. Chem. Soc.* **2001**, *123*, 2018.
(27) Wigner, E. P. Z. *Phys. Chem, B* **1932**, *19*, 203.
(28) Holbrook, K. A.; Pilling, M. J.; Robertson, S. H. *Unimolecular Reactions*; J. Wiley: Chichester, U.K., 1996.
(29) Stein, S. E.; Rabinovitch, B. S. *J. Chem. Phys.* **1973**, *58*, 2438.
(30) Astholz. P. G.; Tore, J.; Wieters, W. *J. Chem. Phys.* **1979**, *70*, 5107.
(31) Gardiner, W. C.; Tore, J. *Combustion Chemistry*; Gardiner, W. C., Ed.; Springer-Verlag: New York, 1994; p 173.
(32) Tore, J. J. *Chem. Phys.* **1977**, *66*, 4758.
(33) Garrett, B. C.; Truhlar, D. G.; Bowman, J. M.; Wagner, A. F.; Robie, D.; Arepalli, S.; Presser, N.; Gordon, R. J. *J. Am. Chem. Soc.* **1986**, *108*, 3515.
(34) Sander, S. P.; Golden, D. M.; Kurylo, M. J.; Orkin, V. L.; Ravishankara, A. R.; Friedl, R. R.; Kolb, C. E.; Molina, M. J.; Moortgat, G. K.; Finlayson-Pitts, B. J.; Huie, R. E. *Chemical Kinetics and Photochemical Data for Use in Stratospheric Modeling*; JPL Publication 02−25; NASA: Pasadena, CA, 2003.